Soils and Rocks

An International Journal of Geotechnical and Geoenvironmental Engineering

www.soilsandrocks.com

ISSN 1980-9743

ISSN-e 2675-5475

Closed-form consolidation solutions for known loading functions

Raphael Felipe Carneiro[1#], Karl Igor Martins Guerra[1], Celso Romanel[1], Denise Maria Soares Gerscovich[2], Bernadete Ragoni Danziger[2]

Technical Note

Keywords
Consolidation
Non-instantaneous loading
Closed-form solution

Abstract

In engineering practice, loading varies with time. However, the classical one-dimensional theory of consolidation assumes the stress increase is instantaneously applied. Many approaches to the problem of time-dependent loading have been proposed over the years, from approximate methods to full developments of differential equations. The paper presents a simple method for finding a closed-form consolidation solution for time-dependent loading without the need for differential equations. Two sets of general equations were derived for both excess pore pressure and average degree of consolidation. Equations were solved for linear, parabolic, sinusoidal, and exponential load functions. Stepped and cyclic loads were also addressed and a numerical solution was developed to verify the obtained result. The method proved to be easy to apply and provides solutions with great simplicity. A case study of non-instantaneous loading on soft clay was also analyzed, and settlement prediction showed good results when compared to readings of the settlement plates.

1. Introduction

Terzaghi & Fröhlich (1936) consolidation theory provides an equation for the excess pore pressure u_z at any depth z and time t, generated by a uniform load q_c. The solution follows:

$$u_z\left(z,T\right) = q_c \sum_{m=0}^{\infty} \frac{2}{M} \sin\frac{Mz}{H_d} e^{-M^2 T} \tag{1}$$

Where

$$M = \left(2m+1\right)\frac{\pi}{2} \tag{2}$$

For m = 1, 2, 3…

And the Time Factor T is defined as:

$$T = \frac{c_v t}{{H_d}^2} \tag{3}$$

The depth-dependent degree of consolidation U_z is given by:

$$U_z\left(z,T\right) = 1 - \sum_{m=0}^{\infty} \frac{2}{M} \sin\frac{Mz}{H_d} e^{-M^2 T} \tag{4}$$

For practical problems, the particular interest is the average degree of consolidation U, given by:

$$U\left(T\right) = 1 - \sum_{m=0}^{\infty} \frac{2}{M^2} e^{-M^2 T} \tag{5}$$

The classical theory uses several simplifying assumptions; among them, the load is instantaneously applied. In practice, however, the increment of total vertical stress often varies with time.

Several empirical and theoretical methods have been proposed to address non-instantaneous load conditions for 1D analyses (Terzaghi & Fröhlich, 1939; Terzaghi, 1943; Schiffman, 1958; Schiffman & Stein, 1970; Zhu & Yin, 1998; Jimenez et al., 2009; Liu & Ma, 2011; Qin et al., 2010; Razouki et al., 2013; Verruijt, 2014; Liu & Griffiths, 2015; Gerscovich et al., 2018).

The ramp loading (Olson, 1977) is the simplest way to address non-instantaneous loading. But some projects impose complex loading sequences. Soil foundations of silos, tanks, highway embankments, etc. undergo cyclic loading. Construction sequences with variable speeds can be represented by non-linear loads.

Hanna et al. (2013) used the concept of discretization of the applied load into infinitesimal increments to easily achieve Olson (1977) solution during construction. Carneiro et al. (2021) demonstrated that Hanna et al. (2013) method is

#Corresponding author. E-mail address: raphaelfc1987@gmail.com
[1]Pontifícia Universidade Católica do Rio de Janeiro, Departamento de Engenharia Civil e Ambiental, Rio de Janeiro, RJ, Brasil.
[2]Universidade do Estado do Rio de Janeiro, Departamento de Estruturas e Fundações, Rio de Janeiro, RJ, Brasil.

Submitted on November 21, 2021; Final Acceptance on December 23, 2022; Discussion open until May 31, 2023.
https://doi.org/10.28927/SR.2023.077721

capable to provide Olson (1977) solution for periods after construction as well. Conte & Troncone (2006) proposed a calculation procedure for a general time-dependent loading, making use of the Fourier series.

This paper presents an extension of and an alternative to the methodologies developed by Conte & Troncone (2006), Hanna et al. (2013), and Carneiro et al. (2021). The solution is a closed-form consolidation equation for different loading functions.

2. Proposed method

In this study, all the simplifying assumptions of the classical theory (Terzaghi & Fröhlich, 1936) are valid. The only exception is the applied vertical load, which is no longer constant but varies up to a Time Factor T_c. All equations for excess pore pressure and degrees of consolidation that refer to non-instantaneous loading are represented below with an apostrophe.

Let the total vertical stress increase $\Delta\sigma(T)$ be a function of T:

$$\Delta\sigma(T) = q(T) \text{ if } T \le T_c \qquad \Delta\sigma(T) = q(T_c) = q_c \text{ if } T > T_c \tag{6}$$

For the purpose of this development, it is assumed that $\Delta\sigma(0) = q(0) = 0$.
Now let $f(T)$ be the derivative of $q(T)$, that is:

$$dq = f(T)\,dT \tag{7}$$

During an infinitesimal dimensionless period dT, the total stress increase $dq = f(T)dT$ is instantaneously applied. Therefore, the initial increase of pore water pressure du_z is also $f(T)dT$. For ramp loads, for example, the load increment ($f(T) = q_c/T_c$) is constant.

As shown in Figure 1, for a Time Factor $T_a \le T_c$ before the end of construction, the infinitesimal loads were applied at an infinite number of times, from $T = 0$ to $T = T_a$. The infinitesimal excess pore pressures dissipate and contribute with dU'_z to compute the degree of consolidation U'_z at the given Time Factor T_a. This infinitesimal increasing of the degree of consolidation dU'_z at T_a is given by the ratio of the dissipated amount of excess pore pressure within the Time Factor interval up to T_a, and the total load.

$$dU'_z(z,T_a) = \frac{dq - du_z(z,T_a - T)}{q_c} = \frac{U_z(z,T_a - T)\,f(T)\,dT}{q_c} \tag{8}$$

Where U_z is given by classical theory (Equation 4).
Considering all time intervals up to T_a, the degree of consolidation U'_z takes into account all infinitesimal loads applied, that is:

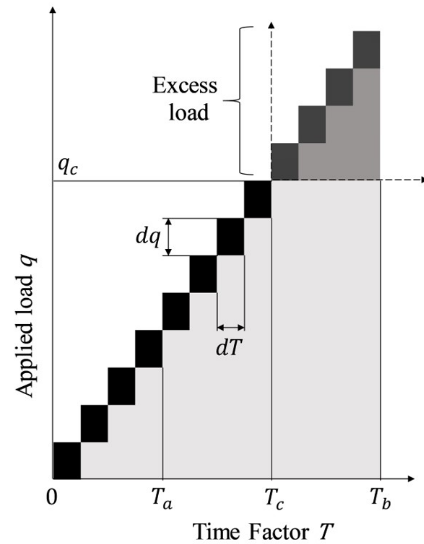

Figure 1. Total stress increase applied into infinitesimal increments [adapted from Hanna et al. (2013), and Carneiro et al. (2021)].

$$U'_z(z,T_a) = \frac{\int_0^{T_a} U_z(z,T_a - T)\,f(T)\,dT}{q_c} \tag{9}$$

Equation 9 holds for any $T_a \le T_c$. This equation is characterized as a convolution of the functions of U_z and f. Solution can be obtained via Laplace transform $\mathcal{L}$:

$$\mathcal{L}\{U'_z\} = \frac{1}{q_c}\mathcal{L}\{U_z\}\mathcal{L}\{f\} \tag{10}$$

Laplace transform of U_z is given by:

$$\mathcal{L}\{U_z\} = \frac{1}{s} - \sum_{m=0}^{\infty}\left(\frac{2}{M}\right)\left(\sin\frac{Mz}{H_d}\right)\frac{1}{s+M^2} \tag{11}$$

Where s is the Laplace parameter.
Denoting $\mathcal{L}\{f\} = F(s)$, Equation 10 can now be rewritten as:

$$\mathcal{L}\{U'_z\} = \frac{1}{q_c}\left[\frac{F(s)}{s} - \sum_{m=0}^{\infty}\left(\frac{2}{M}\right)\left(\sin\frac{Mz}{H_d}\right)\frac{F(s)}{s+M^2}\right] \tag{12}$$

Applying the inverse Laplace transform, one has:

$$U'_z(T) = \frac{q(T)}{q_c} - \frac{1}{q_c}\sum_{m=0}^{\infty}\left(\frac{2}{M}\right)\left(\sin\frac{Mz}{H_d}\right)\mathcal{L}^{-1}\left\{\frac{F(s)}{s+M^2}\right\}\Bigg|_0^T \tag{13}$$

After the end of construction, for a Time Factor $T_b \ge T_c$ shown in Figure 1, solution uses the principle of superposition. The degree of consolidation at a Time Factor T_b is calculated by subtracting the exceeding loading, calculated as if the time-dependent loading has not finished, from the actual final value q_c.

Thus, the degree of consolidation is calculated by:

$$U'_z\left(T_b\right)=U'_{z1}\left(T_b\right)-U'_{z2}\left(T_b\right) \quad (14)$$

The expression of U'_{z1} is given by Equation 13 for $T = T_b$. For U'_{z2}, the origin is now at T_c, thus $T = T_b - T_c$. So, Equation 9 must be rewritten as follows:

$$U'_{z2}\left(T_b\right)=\frac{\int_0^{T_b-T_c} U_z\left(T_b-T_c-T\right) f\left(T+T_c\right) dT}{q_c} \quad (15)$$

Denoting the shifted function $f(T + T_c) = g(T)$, Equation 15 is the convolution of U_z and g. Applying the Laplace transform:

$$\mathcal{L}\left\{U'_{z2}\right\}=\frac{1}{q_c}\left[\frac{G(s)}{s}-\sum_{m=0}^{\infty}\left(\frac{2}{M}\right)\left(\sin\frac{Mz}{H_d}\right)\frac{G(s)}{s+M^2}\right] \quad (16)$$

Where $G\left(s\right)=\mathcal{L}\left\{g\right\}$. Applying the inverse Laplace transform, the solution is:

$$U'_{z2}\left(T_b\right)=\frac{q\left(T_b\right)}{q_c}-1-\frac{1}{q_c}\sum_{m=0}^{\infty}\left(\frac{2}{M}\right)\left(\sin\frac{Mz}{H_d}\right)\mathcal{L}^{-1}\left\{\frac{G(s)}{s+M^2}\right\}\Bigg|_0^{T_b-T_c} \quad (17)$$

Finally, Equation 14 can be expressed as:

$$U'_z(T)=1-\frac{1}{q_c}\sum_{m=0}^{\infty}\left(\frac{2}{M}\right)\left(\sin\frac{Mz}{H_d}\right)\left[\mathcal{L}^{-1}\left\{\frac{F(s)}{s+M^2}\right\}\Bigg|_0^{T}-\mathcal{L}^{-1}\left\{\frac{G(s)}{s+M^2}\right\}\Bigg|_0^{T-T_c}\right] \quad (18)$$

Equations 13 and 18 provide the degree of consolidation for periods before and after the end of construction, respectively. For any loading function $q(T)$, its derivative $f(T)$ and the function $g(T) = f(T + T_c)$ are known. Once $F(s)$ and $G(s)$ are determined, solution is obtained. Equations 13 and 18 are coincident for $T = T_c$.

From Equations 13 and 18, the excess pore pressure can be found:

$$u'_z(T)=\sum_{m=0}^{\infty}\left(\frac{2}{M}\right)\left(\sin\frac{Mz}{H_d}\right)\mathcal{L}^{-1}\left\{\frac{F(s)}{s+M^2}\right\}\Bigg|_0^{T} \text{ if } T\le T_c$$

$$u'_z(T)=\sum_{m=0}^{\infty}\left(\frac{2}{M}\right)\left(\sin\frac{Mz}{H_d}\right)\left[\mathcal{L}^{-1}\left\{\frac{F(s)}{s+M^2}\right\}\Bigg|_0^{T}-\mathcal{L}^{-1}\left\{\frac{G(s)}{s+M^2}\right\}\Bigg|_0^{T-T_c}\right] \text{ if } T>T_c \quad (19)$$

The average degree of consolidation U' provides the sum of the vertical compressions throughout the depth, and it is calculated by:

$$U'\left(T\right)=\frac{\int_0^{2H_d} U'_z\left(z,T\right)dz}{\int_0^{2H_d} dz} \quad (20)$$

Which gives:

$$U'\left(T\right)=\frac{q\left(T\right)}{q_c}-\frac{1}{q_c}\sum_{m=0}^{\infty}\left(\frac{2}{M^2}\right)\mathcal{L}^{-1}\left\{\frac{F(s)}{s+M^2}\right\}\Bigg|_0^{T} \text{ if } T\le T_c$$

$$U'(T)=1-\frac{1}{q_c}\sum_{m=0}^{\infty}\left(\frac{2}{M^2}\right)\left[\mathcal{L}^{-1}\left\{\frac{F(s)}{s+M^2}\right\}\Bigg|_0^{T}-\mathcal{L}^{-1}\left\{\frac{G(s)}{s+M^2}\right\}\Bigg|_0^{T-T_c}\right] \text{ if } T>T_c \quad (21)$$

While the loading in Figure 1 was represented as linear for simplification, the mathematical development allows to find general equations to compute the excess pore pressure (Equation 18) and the average degree of consolidation (Equation 21) for any loading function.

3. Applications

This section presents several applications of the equations. Calculations are detailed in Appendix 1.

Since the development was based on the simplifying assumptions of the classical theory, the solutions herein presented are limited to uniform initial excess pore pressure. The drainage conditions can be single or double.

3.1 Single ramp load

The consolidation theory for an increasing linear loading was primarily solved by Terzaghi & Fröhlich (1939), and later by Olson (1977). The function $q(T)$ is given by $q(T) = \frac{q_c}{T_c}T$, and, therefore, $f(T) = \frac{q_c}{T_c}$ is a constant. The solution of Equations 19 and 21 give the excess pore pressure and the average degree of consolidation before and after construction. It worth mentioning that the solutions coincide with Olson (1977).

$$u'_z\left(T\le T_c\right)=\frac{q_c}{T_c}\sum_{m=0}^{\infty}\left(\frac{2}{M^3}\right)\left(\sin\frac{Mz}{H_d}\right)\left[1-e^{-M^2T}\right]$$

$$U'\left(T\le T_c\right)=\frac{T}{T_c}-\frac{1}{T_c}\sum_{m=0}^{\infty}\left(\frac{2}{M^4}\right)\left[1-e^{-M^2T}\right]$$

$$u'_z\left(T>T_c\right)=\frac{q_c}{T_c}\sum_{m=0}^{\infty}\left(\frac{2}{M^3}\right)\left(\sin\frac{Mz}{H_d}\right)\left[e^{-M^2\left(T-T_c\right)}-e^{-M^2T}\right]$$

$$U'\left(T>T_c\right)=1-\frac{1}{T_c}\sum_{m=0}^{\infty}\left(\frac{2}{M^4}\right)\left[e^{-M^2\left(T-T_c\right)}-e^{-M^2T}\right] \quad (22)$$

3.2 Multiple ramp load

Embankments are typical examples of multiple ramp load constructions. The loading rate and the time interval between load sequences vary. The final load is achieved after n ramp loads intercalated with $n - 1$ pause periods. The end of construction corresponds to the n-th pause period. As illustrated in Figure 2, each ramp load may have a different inclination α_i, with i varing from 1 to n.

Assuming that the Time Factor at the beginning of a ramp load is defined as T_{2i-2}, and T_{2i-1} is the corresponding value at its end (or at the beginning of a pause period), the derivative $f(T)$ of the loading function $q(T)$ can be expressed as:

$$f\left(T\right)=\sum_{i=1}^{n}\alpha_i\mathcal{H}\left(T-T_{2i-2}\right)-\alpha_i\mathcal{H}\left(T-T_{2i-1}\right) \tag{23}$$

Where the Heaviside function $\mathcal{H}\left(T\right)$ yields zero or one, depending on the argument be negative or positive.

For simplification, it is beneficial to consider that the n-th pause period is still part of the construction, and the end of construction occurs at $T_c = T_{2n} \rightarrow \infty$. It is an equivalent configuration that allows using only one equation for the average degree of consolidation instead of two, since $g(T)$ is no longer needed.

Thus, the average degree of consolidation is:

$$U'\left(T\right)=\frac{q\left(T\right)}{q_c}-\frac{1}{q_c}\sum_{m=0}^{\infty}\left(\frac{2}{M^4}\right)\sum_{i=1}^{n}\alpha_i\left\{\begin{matrix}\left[1-\mathrm{e}^{-M^2\left(T-T_{2i-2}\right)}\right]\mathcal{H}\left(T-T_{2i-2}\right)- \\ \left[1-\mathrm{e}^{-M^2\left(T-T_{2i-1}\right)}\right]\mathcal{H}\left(T-T_{2i-1}\right)\end{matrix}\right\} \tag{24}$$

For $n = 1$, Equation 24 coincides with Olson (1977) solution during and after construction. In this scenario, $T_1 = T_c$ and $\alpha_i = \frac{q_c}{T_c}$. For $n > 1$, it coincides with Olson (1977) proposition of adding the solutions for each ramp load.

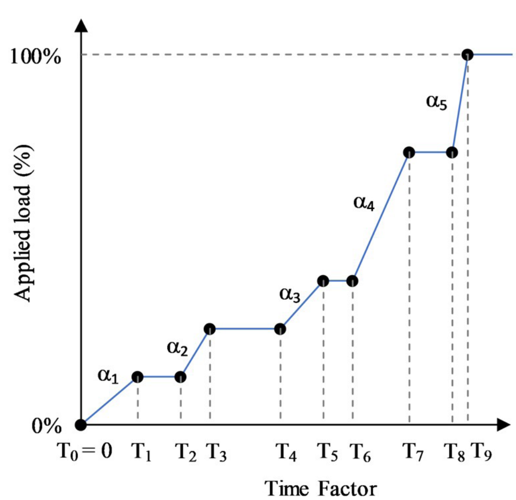

Figure 2. Construction sequence with $n = 5$ ramp loads.

3.3 Other single load functions

In some geotechnical problems, like embankments built at a given rate, loading sequences can be better reproduced by non-linear loads, depending on the speed of construction. Jimenez et al. (2009) studied parabolic loading for vertical and radial consolidation combined. Qin et al. (2010) studied exponential loading for unsaturated soil.

In the case of a quadratic function (parabola), the loading is given by

$$q\left(T\right)=\frac{q_c}{T_c^{\,2}}T^2 \tag{25}$$

Now the rate of loading is no longer constant, since $f(T) = \frac{2q_c}{T_c^2}T$, and the shifted function is $f(T) = \frac{2q_c}{T_c^2}(T + T_c)$.

Combining Equation 21 to Equation 25, the average degree of consolidation is expressed by:

$$\begin{aligned}U'\left(T\le T_c\right)&=\frac{T^2}{T_c^{\,2}}-\frac{1}{T_c^{\,2}}\sum_{m=0}^{\infty}\left(\frac{4}{M^6}\right)\left[M^2T-1+e^{-M^2T}\right]\\ U'\left(T>T_c\right)&=1-\frac{1}{T_c^{\,2}}\sum_{m=0}^{\infty}\left(\frac{4}{M^6}\right)\left[\left(M^2T_c-1\right)e^{-M^2\left(T-T_c\right)}+e^{-M^2T}\right]\end{aligned} \tag{26}$$

If the loading is better reproduced in the form of a sinusoidal function until the end of the construction, that load can be represented by:

$$q\left(T\right)=q_c\sin\left(\frac{\pi}{2T_c}T\right) \tag{27}$$

The rate of loading is therefore $f(T) = \frac{\pi}{2T_c}q_c\cos\left(\frac{\pi}{2T_c}T\right)$ and the shifted function is $g(T) = -\frac{\pi}{2T_c}q_c\sin\left(\frac{\pi}{2T_c}T\right)$.

Substituting these equations into Equation 21, the solution for U' is given by:

$$\begin{aligned}U'\left(T\le T_c\right)&=\sin\left(\frac{\pi}{2T_c}T\right)-\frac{\pi}{2T_c}\sum_{m=0}^{\infty}\frac{2}{M^4+\left(\frac{\pi}{2T_c}\right)^2}\\ &\left[\frac{1}{M^2}\frac{\pi}{2T_c}\sin\left(\frac{\pi}{2T_c}T\right)+\cos\left(\frac{\pi}{2T_c}T\right)-e^{-M^2T}\right]\\ U'\left(T>T_c\right)&=1-\frac{\pi}{2T_c}\sum_{m=0}^{\infty}\frac{2}{M^4+\left(\frac{\pi}{2T_c}\right)^2}\left[\frac{1}{M^2}\frac{\pi}{2T_c}e^{-M\ \left(T-T_c\right)}-e^{-M\ T}\right]\end{aligned} \tag{28}$$

In the case of exponential load function, the load expression is:

$$q\left(T\right)=\frac{q_c}{1-e^{-\beta T_c}}\left(1-e^{-\beta T}\right) \tag{29}$$

For this loading condition, the average degree of consolidation is expressed by:

$$\begin{gathered}U'\left(T\le T_c\right)=\left(\frac{1-e^{-\beta T}}{1-e^{-\beta T_c}}\right)-\frac{\beta}{1-e^{-\beta T_c}}\sum_{m=0}^{\infty}\left(\frac{2}{M^2}\right)\left(\frac{1}{M^2-\beta}\right)\left[e^{-\beta T}-e^{-M^2T}\right]\\ U'\left(T>T_c\right)=1-\frac{\beta}{1-e^{-\beta T_c}}\sum_{m=0}^{\infty}\left(\frac{2}{M^2}\right)\left(\frac{1}{M^2-\beta}\right)\left[e^{-M^2\left(T-T_c\right)-\beta T_c}-e^{-M^2T}\right]\end{gathered} \tag{30}$$

Equation 29 is able to reproduce other loading conditions. At the upper limit ($\beta \rightarrow \infty$), the equation is equivalent to an instantaneous load applied at T = 0. On the other hand, if $\beta \rightarrow -\infty$ the equivalence occurs as if the instantaneous load was applied at $T = T_c$. If $\beta \rightarrow 0.$, the equation reproduces a ramp load.

Figure 3 compares the average degree of consolidation versus Time Factor for different loading conditions. The end of construction was set at T_c = 0.126 for all non-instantaneous loads. The exponential function was analyzed for β = 40 and β = −40 (Equation 29).

In the upper part of Figure 3, the time-dependent loads are shown. Exponential (β = 40) and sinusoidal loading indicate higher speed at the beginning of construction. Exponential (β = −40) and parabolic loading indicate higher speed at the end of construction. The results showed consistency: the greater the rate of loading the faster the consolidation.

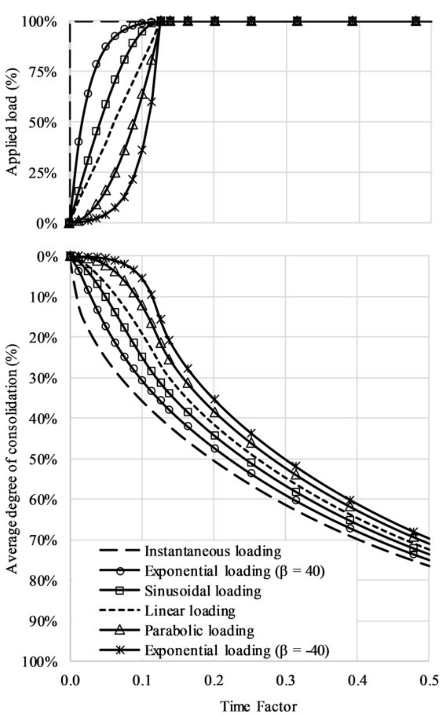

Figure 3. Consolidation curves for parabolic, sinusoidal, exponential, instantaneous and linear loading.

The influence of the construction sequence on the degree of consolidation decreases with time. However, during the construction period, there is a significant difference among the curves. In the comparison shown in Figure 3, the absolute difference between the average degrees of consolidation of both exponential loadings at the end of construction is around 20%.

3.4 Haversine repeated load

Several geotechnical engineering phenomena can produce repeated or cyclic loading, such as vehicular traffic, wind waves, sea waves, etc. (Mitchell, 1993). Huang (1993) studied the influence of the wheel load on highways and airports and proposed the use of a haversine repeated loading given by:

$$q\left(T\right)=q_c\sin^2\left(\frac{\pi}{\tau}T\right) \tag{31}$$

Equation 31 assumes that the loading-unloading sequence does not reach an end; that is, the "end of construction" is at infinity. Thus, q_c should now be interpreted as the load amplitude, and the excess pore pressure can only be calculated for $T \le T_c$. Since the derivative of $q(T)$ is $f(T)=q_c\frac{\pi}{\tau}\sin\left(\frac{2\pi}{\tau}T\right)$, the excess pore pressure (Equation 19) is solved and agrees with Razouki et al. (2013) solution:

$$\begin{gathered}u'_z\left(T\right)=q_c\sum_{m=0}^{\infty}\left[\frac{\left(\frac{2\pi}{\tau}\right)^2}{\left(\frac{2\pi}{\tau}\right)^2M+M^5}\right]\left(\sin\frac{Mz}{H_d}\right)\\ \left[e^{-M^2T}-\cos\left(\frac{2\pi}{\tau}T\right)+\frac{M^2}{\left(\frac{2\pi}{\tau}\right)}\sin\left(\frac{2\pi}{\tau}T\right)\right]\end{gathered} \tag{32}$$

Results for τ = 0.15 are presented in Figure 4. The upper part shows the time-dependent load. The lower part compares the analytical solution, obtained by the present method and by Razouki et al. (2013), with Razouki & Schanz (2011) numerical solution.

3.5 Damped cyclic load

The damped cyclic load may be generated by an instantaneous load that causes a damped oscillation of the applied stress. As shown in Figure 5, the waves have higher amplitude at the beginning, and converge to a residual load after some oscillations.

This loading condition can be represented by a product of functions, such as:

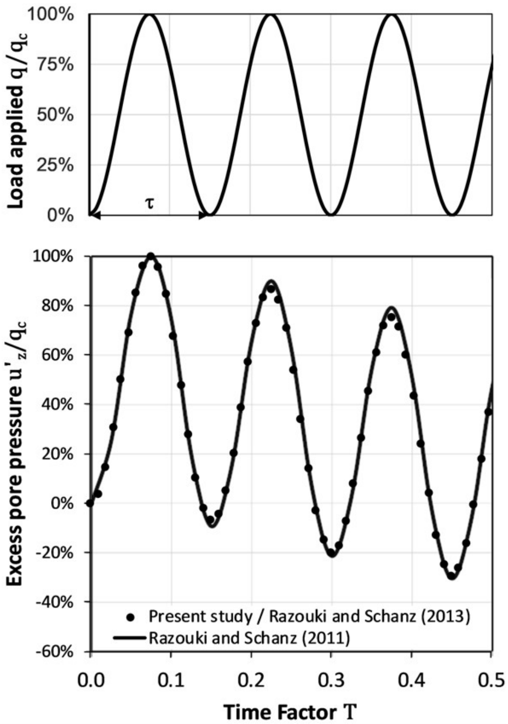

Figure 4. Normalized excess pore pressure versus time factor for the Haversine repeated load [adapted from Razouki & Schanz (2011)].

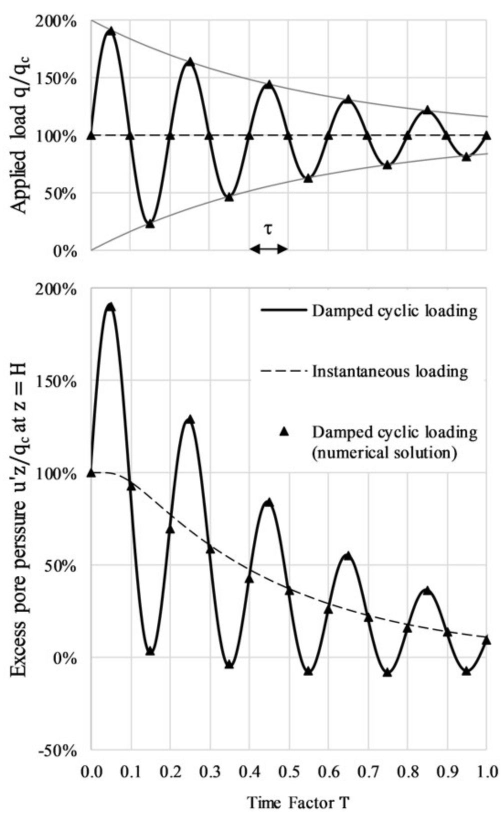

Figure 5. Variation of excess pore pressure due to a damped cyclic loading.

$$q(T) = q_c\left[1 + e^{-\beta T}\sin\left(\frac{\pi}{\tau}T\right)\right] \tag{33}$$

Since there is load being applied instantaneously, it is convenient to separate the function into two parts: i) instantaneous and ii) time-dependent. The instantaneous load is governed by classical theory, while the time-dependent load is obtained by the method herein proposed. In this case, the time-dependent function is given by:

$$q(T) = q_c\left[e^{-\beta T}\sin\left(\frac{\pi}{\tau}\bullet T\right)\right] \tag{34}$$

Similar to the previous example, the solution is only needed for $T \leq T_c$. Combining Equation 34 with Equation 19, the time dependent solution is given by:

$$\frac{u'_z(T)}{q_c} = \sum_{m=0}^{\infty}\frac{2}{M}\left(\sin\frac{Mz}{H_d}\right)\left[Xe^{-\beta T}\cos\left(\frac{\pi}{\tau}T\right) + Ye^{-\beta T}\sin\left(\frac{\pi}{\tau}T\right) - Xe^{-M^2T}\right] \tag{35}$$

And the final solution, combined with the classical theory (Terzaghi & Fröhlich, 1936) to include the instantaneous load part, is expressed by:

$$\frac{u'_z(T)}{q_c} = \sum_{m=0}^{\infty}\frac{2}{M}\left(\sin\frac{Mz}{H_d}\right)\left[Xe^{-\beta T}\cos\left(\frac{\pi}{\tau}T\right) + Ye^{-\beta T}\sin\left(\frac{\pi}{\tau}T\right) + (1-X)e^{-M^2T}\right] \tag{36}$$

Where:

$$X = \frac{\left(\frac{\pi}{\tau}\right)M^2}{\beta^2 + \left(\frac{\pi}{\tau}\right)^2 - 2\beta M^2 + M^4}$$
$$Y = \frac{\beta^2 + \left(\frac{\pi}{\tau}\right)^2 - \beta M^2}{\beta^2 + \left(\frac{\pi}{\tau}\right)^2 - 2\beta M^2 + M^4} \tag{37}$$

The solution was applied to a hypothetical example, consisting of a damped cyclic load on a single drainage clay deposit. The parameters of this cyclic loading (Equation (34)) are $\beta = 1.8$ and $\tau = 0.1$. Figure 5 shows the normalized excess pore pressure (u'_z/q_c) at the bottom of the clay deposit ($z = H$). As expected, the excess pore pressure tends to hover around Terzaghi & Fröhlich (1936) solution over time (Equation 1).

A numerical finite difference solution was developed to solve the governing differential equation, in order to verify the behavior of the consolidation process. The thickness was divided so that each subdivision measured 0.005. A dimensionless time interval of 0.05 was adopted. It can be seen in Figure 5 that there is a great agreement between analytical (Equation 36) and numerical solution.

It can be noticed that the excess pore pressure eventually becomes negative due to the loading-unloading sequence. Negative excess pore pressure is a common issue in cyclic loading cases (Razouki & Schanz, 2011). That phenomenon is controlled by β, so the smaller the β value, the more negative the excess pore pressure during the unloading phases.

4. Case study

Nascimento (2016) describes a case of an instrumented experimental embankment built on soft soil in Macaé, Rio de Janeiro. The clay layer is 7.85 meters thick, double-drained, and laboratory tests provided a coefficient of consolidation of 10^{-7} m^2/s.

The embankment reached a final height of 3.1 m in about 1 month. For the present study, the construction sequence was approximated to an exponential (Equation 29) with $\beta = 80$, as shown in the upper part of Figure 6. Nascimento (2016) estimated an immediate settlement of 0.15 m, and a primary settlement of 2.16 m.

The settlement estimate was compared with the readings of settlement plates, in the lower part of Figure 6. Immediate settlement was distributed over the construction period in proportion to the calculated embankment height. The results show a good approximation between settlement estimate and plate readings.

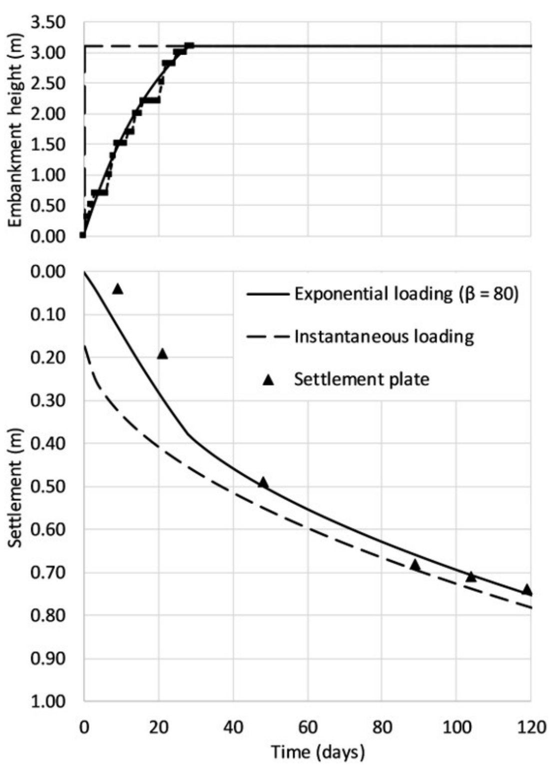

Figure 6. Settlement prediction for Macaé clay (Nascimento, 2016) with a construction sequence approximated to an exponential.

5. Conclusions

This study presented a closed-form consolidation solution for a time-dependent loading function. Two sets of equations were established to determine the excess pore pressure and the average degree of consolidation during construction and after construction.

The method is easy to apply and does not require the development of any differential equation. Solutions for single load functions (linear, parabolic, sinusoidal and exponential) and cyclic loads (haversine and damped) were presented. Results were consistent with the physical consolidation phenomena and agreed with some known analytical solutions and also with a numerical solution.

A case study with an approximately exponential construction sequence was analyzed. A comparison between the settlement plate readings and the solution proposed in the present paper was made, with good results.

Acknowledgements

The authors thank the Brazilian research agency CAPES and the Pontifical Catholic University of Rio de Janeiro (PUC-Rio) for their support.

Declaration of interest

The authors have no conflicts of interest to declare. All co-authors have observed and affirmed the contents of the paper and there is no financial interest to report.

Authors' contributions

Raphael Felipe Carneiro: conceptualization, data curation, formal analysis, investigation, methodology, validation, writing – original draft. Karl Igor Martins Guerra: data curation, formal analysis, investigation, validation. Celso Romanel: supervision, validation, writing – review & editing. Denise Maria Soares Gerscovich: visualization, writing – review & editing. Bernadete Ragoni Danziger: visualization, writing – review & editing.

Data availability

All data produced or examined in the course of the current study are included in this article.

List of symbols

c_v coefficient of consolidation
f rate of loading function
g shifted rate of loading function
i index
m count parameter

n	number of ramp loads
q	load function
q_c	total load
s	Laplace parameter
t	time
u_z	excess pore pressure for instantaneous loading
u'_z	excess pore pressure for time-dependent loading
z	depth
F	Laplace transform of f
G	Laplace transform of g
H	total thickness of the clay layer
H_d	maximum length of drainage path
M	count parameter
T	time factor
T_a	time factor before the end of construction
T_b	time factor after the end of construction
T_c	time factor at the end of construction
U	average degree of consolidation for instantaneous loading
U''	average degree of consolidation for a time-dependent loading
U_z	depth-variable degree of consolidation for instantaneous loading
U'_z	depth-variable degree of consolidation for a time-dependent loading
α	inclination of a ramp load
β	fit parameter
$\Delta\sigma$	total vertical stress increase
τ	dimensionless half-period of a sinusoid function

References

Carneiro, R., Gerscovich, D., & Danziger, B. (2021). A simple approach to predict settlement due to constant rate loading in clays. *Soils and Rocks*, *44*(2), 1-8. http://dx.doi.org/10.28927/SR.2021.057120.

Conte, E., & Troncone, A. (2006). One-dimensional consolidation under general time-dependent loading. *Canadian Geotechnical Journal*, *43*(11), 1107-1116. http://dx.doi.org/10.1139/t06-064.

Gerscovich, D., Carneiro, R., & Danziger, B. (2018). Extension of Terzaghi's graphical method to predict settlement due to stepped load. *International Journal of Geomechanics*, *18*(12), 06018033. http://dx.doi.org/10.1061/(ASCE)GM.1943-5622.0001266.

Hanna, D., Sivakugan, N., & Lovisa, J. (2013). Simple approach to consolidation due to constant rate loading in clays. *International Journal of Geomechanics*, *13*(2), 193-196. http://dx.doi.org/10.1061/(ASCE)GM.1943-5622.0000195.

Huang, Y.H. (1993). *Pavement analysis and design*. Prentice-Hall.

Jimenez, R.R., Serrano, G.A., & Olalla, M.C. (2009). Consolidation charts for non-linearly time-increasing loads. *Proceedings of the Institution of Civil Engineers - Ground Improvement*, 162(2), 103-108. http://dx.doi.org/10.1680/grim.2009.162.2.103.

Liu, J., & Ma, Q. (2011). One-dimensional consolidation of soft ground with impeded boundaries under depth-dependent ramp load. In B. Huang, B.F. Bowers, G.-X. Mei, S.-H. Luo & Z. Zhang (Eds.), *Pavement and geotechnical engineering for transportation* (pp. 127-134). American Society of Civil Engineers. https://doi.org/10.1061/9780784412817.015.

Liu, J.C., & Griffiths, D. (2015). A general solution for 1D consolidation induced by depth- and time-dependent changes in stress. *Geotechnique*, *65*(1), 66-72. http://dx.doi.org/10.1680/geot.14.P.077.

Mitchell, J.K. (1993). *Fundamentals of soil behavior*. Wiley.

Nascimento, P.N.C. (2016). *Analysis of an experimental embankment led to failure located in Macaé - RJ* [Master's dissertation]. State University of Northern Rio de Janeiro – UENF. (in Portuguese).

Olson, R. (1977). Consolidation under time dependence loading. *Journal of the Geotechnical Engineering Division*, *103*(1), 55-60. http://dx.doi.org/10.1061/AJGEB6.0000369.

Qin, A.F., Sun, D.A., & Tan, Y.W. (2010). Analytical solution to one-dimensional consolidation in unsaturated soils under loading varying exponentially with time. *Computers and Geotechnics*, *37*(1-2), 233-238. http://dx.doi.org/10.1016/j.compgeo.2009.07.008.

Razouki, S.S., & Schanz, T. (2011). One-dimensional consolidation under haversine repeated loading with rest period. *Acta Geotechnica*, *6*(1), 13-20. http://dx.doi.org/10.1007/s11440-010-0132-1.

Razouki, S.S., Bonnier, P., Datcheva, M., & Schanz, T. (2013). Analytical solution for 1D consolidation under haversine cyclic loading. *International Journal for Numerical and Analytical Methods in Geomechanics*, *37*(14), 2367-2372. http://dx.doi.org/10.1002/nag.2188.

Schiffman, R.L. (January 6-10, 1958). Consolidation of soil under time dependent loading and varying permeability. In H.P. Orland (Ed.), *Proceedings of the Thirty-Seventh Annual Meeting of the Highway Research Board* (pp. 584-615). Washington DC, United States of America: Highway Research Board.

Schiffman, R.L., & Stein, J.R. (1970). One-dimensional consolidation of layered systems. *Journal of the Soil Mechanics and Foundations Division*, *96*(SM4), 1499-1504. http://dx.doi.org/10.1061/JSFEAQ.0001453.

Terzaghi, K. (1943). *Theoretical soil mechanics*. Wiley.

Terzaghi, K.F., & Fröhlich, O.K. (1936). *Theorie der setzung von tonschichten*. Franz Deuticke. In German.

Terzaghi, K.F., & Fröhlich, O.K. (1939). *Théorie du tassement des couches argileuses: introduction à la mécanique analytique des argiles*. Dunod. In French.

Verruijt, A. (2014). *Theory and problems of poroelasticity*. Delft University of Technology.

Zhu, G., & Yin, J. (1998). Consolidation of soil under depth-dependent ramp load. *Canadian Geotechnical Journal*, *35*(2), 344-350. http://dx.doi.org/10.1139/t97-092.

Appendix 1. Laplace Transform calculations.

The following equations were used during the development of the solutions presented in this study. The terms $\frac{F(s)}{s+M^2}$ and $\frac{G(s)}{s+M^2}$ are already rewritten as a sum of fractions.

▪ Ramp load

$$\begin{aligned}
&f(T)=g(T)=\frac{q_c}{T_c}\\
&F(s)=G(s)=\frac{q_c}{T_c}\frac{1}{s}\\
&\frac{F(s)}{s+M^2}=\frac{G(s)}{s+M^2}=\frac{q_c}{T_c}\frac{1}{M^2}\left(\frac{1}{s}-\frac{1}{s+M^2}\right)\\
&\mathcal{L}^{-1}\left\{\frac{F(s)}{s+M^2}\right\}=\mathcal{L}^{-1}\left\{\frac{G(s)}{s+M^2}\right\}=\frac{q_c}{T_c}\frac{1}{M^2}\left(1-e^{-M^2T}\right)
\end{aligned} \tag{38}$$

▪ Multiple ramp loads

$$\begin{aligned}
&f(T)=\sum_{i=1}^{n}\alpha_i\mathcal{H}(T-T_{2i-2})-\alpha_i\mathcal{H}(T-T_{2i-1})\\
&F(s)=\sum_{i=1}^{n}\alpha_i\frac{\exp(-sT_{2i-2})}{s}-\alpha_i\frac{\exp(-sT_{2i-1})}{s}\\
&\frac{F(s)}{s+M^2}=\sum_{i=1}^{n}\frac{\alpha_i}{M^2}\left[\exp(-sT_{2i-2})\left(\frac{1}{s}-\frac{1}{s+M^2}\right)-\exp(-sT_{2i-1})\left(\frac{1}{s}-\frac{1}{s+M^2}\right)\right]\\
&\mathcal{L}^{-1}\left\{\frac{F(s)}{s+M^2}\right\}=\sum_{i=1}^{n}\frac{\alpha_i}{M^2}\left\{\left\{1-\exp\left[-M^2(T-T_{2i-2})\right]\right\}\mathcal{H}(T-T_{2i-2})-\left\{1-\exp\left[-M^2(T-T_{2i-1})\right]\right\}\mathcal{H}(T-T_{2i-1})\right\}
\end{aligned} \tag{39}$$

▪ Parabolic load

$$\begin{aligned}
&f(T)=2\frac{q_c}{T_c^2}T\\
&F(s)=2\frac{q_c}{T_c^2}\frac{1}{s^2}.\\
&\frac{F(s)}{s+M^2}=2\frac{q_c}{T_c^2}\frac{1}{M^4}\left(\frac{1}{s+M^2}-\frac{1}{s}+M^2\frac{1}{s^2}\right)\\
&\mathcal{L}^{-1}\left\{\frac{F(s)}{s+M^2}\right\}=2\frac{q_c}{T_c^2}\frac{1}{M^4}\left(e^{-M^2T}-1+M^2T\right)\\
&G(s)=2\frac{q_c}{T_c^2}\left(\frac{1}{s^2}+T_c\frac{1}{s}\right)\\
&\frac{G(s)}{s+M^2}=2\frac{q_c}{T_c^2}\left[\frac{1}{M^4}\left(\frac{1}{s+M^2}-\frac{1}{s}+M^2\frac{1}{s^2}\right)+\frac{T_c}{M^2}\left(\frac{1}{s}-\frac{1}{s+M^2}\right)\right].\\
&\mathcal{L}^{-1}\left\{\frac{G(s)}{s+M^2}\right\}=2\frac{q_c}{T_c^2}\left[\frac{1}{M^4}\left(e^{-M^2T}-1+M^2T\right)+\frac{T_c}{M^2}\left(1-e^{-M^2T}\right)\right]
\end{aligned} \tag{40}$$

▪ Sinusoidal load

$$f(T) = \frac{\pi}{2T_c} q_c \cos\left(\frac{\pi}{2T_c} T\right)$$

$$F(s) = \frac{\pi}{2T_c} q_c \frac{s}{s^2 + \left(\frac{\pi}{2T_c}\right)^2}$$

$$\frac{F(s)}{s+M^2} = \frac{\frac{\pi}{2T_c} q_c}{M^4 + \left(\frac{\pi}{2T_c}\right)^2} \left(\frac{\pi}{2T_c} \frac{\frac{\pi}{2T_c}}{s^2 + \left(\frac{\pi}{2T_c}\right)^2} + M^2 \frac{s}{s^2 + \left(\frac{\pi}{2T_c}\right)^2} - M^2 \frac{1}{s+M^2} \right)$$

$$\mathcal{L}^{-1}\left\{\frac{F(s)}{s+M^2}\right\} = \frac{\frac{\pi}{2T_c} q_c}{M^4 + \left(\frac{\pi}{2T_c}\right)^2} \left[\frac{\pi}{2T_c} \sin\left(\frac{\pi}{2T_c} T\right) + M^2 \cos\left(\frac{\pi}{2T_c} T\right) - M^2 e^{-M^2 T} \right]$$

$$g(T) = \frac{\pi}{2T_c} q_c \cos\left[\frac{\pi}{2T_c}(T + T_c)\right] = -\frac{\pi}{2T_c} q_c \left[\sin\left(\frac{\pi}{2T_c} T\right)\right] \tag{41}$$

$$G(s) = -\frac{\pi}{2T_c} q_c \frac{\frac{\pi}{2T_c}}{s^2 + \left(\frac{\pi}{2T_c}\right)^2}$$

$$\frac{G(s)}{s+M^2} = \frac{-\frac{\pi}{2T_c} q_c}{M^4 + \left(\frac{\pi}{2T_c}\right)^2} \left[M^2 \frac{\frac{\pi}{2T_c}}{s^2 + \left(\frac{\pi}{2T_c}\right)^2} - \frac{\pi}{2T_c} \frac{s}{s^2 + \left(\frac{\pi}{2T_c}\right)^2} + \frac{\pi}{2T_c} \frac{1}{s+M^2} \right]$$

$$\mathcal{L}^{-1}\left\{\frac{G(s)}{s+M^2}\right\} = \frac{-\frac{\pi}{2T_c} q}{M^4 + \left(\frac{\pi}{2T_c}\right)^2} \left[M^2 \sin\left(\frac{\pi}{2T_c} T\right) - \frac{\pi}{2T_c} \cos\left(\frac{\pi}{2T_c} T\right) + \frac{\pi}{2T_c} e^{-M^2 T} \right]$$

▪ Exponential load

$$f(T) = \frac{q_c}{1 - e^{-\beta T_c}} \beta e^{-\beta T}$$

$$F(s) = \frac{q_c}{1 - e^{-\beta T_c}} \beta \frac{1}{s + \beta}$$

$$\frac{F(s)}{s + M^2} = \frac{q_c}{1 - e^{-\beta T_c}} \left(\frac{\beta}{M^2 - \beta} \right) \left(\frac{1}{s + \beta} - \frac{1}{s + M^2} \right)$$

$$\mathcal{L}^{-1} \left\{ \frac{F(s)}{s + M^2} \right\} = \frac{q_c}{1 - e^{-\beta T_c}} \left(\frac{\beta}{M^2 - \beta} \right) \left(e^{-\beta T} - e^{-M^2 T} \right)$$

$$g(T) = \frac{q_c}{1 - e^{-\beta T_c}} \beta e^{-\beta(T + T_c)} = -\frac{q_c}{1 - e^{-\beta T_c}} \beta e^{-\beta T_c} e^{-\beta T} \tag{42}$$

$$G(s) = \frac{q_c}{1 - e^{-\beta T_c}} \beta e^{-\beta T_c} \frac{1}{s + \beta}$$

$$\frac{G(s)}{s + M^2} = -\frac{q_c}{1 - e^{-\beta T_c}} \left(\frac{\beta e^{-\beta T_c}}{M^2 - \beta} \right) \left(\frac{1}{s + \beta} - \frac{1}{s + M^2} \right)$$

$$\mathcal{L}^{-1} \left\{ \frac{G(s)}{s + M^2} \right\} = -\frac{q_c}{1 - e^{-\beta T_c}} \left(\frac{\beta e^{-\beta T_c}}{M^2 - \beta} \right) \left(e^{-\beta T} - e^{-M^2 T} \right)$$

▪ Haversine repeated load

$$f(T) = q_c \frac{\pi}{\tau} \sin\left(\frac{2\pi}{\tau} T \right)$$

$$F(s) = q_c \frac{\pi}{\tau} \frac{\frac{2\pi}{\tau}}{s^2 + \left(\frac{2\pi}{\tau} \right)^2} = 2 q_c \left(\frac{\pi}{\tau} \right)^2 \frac{1}{s^2 + \left(\frac{2\pi}{\tau} \right)^2}$$

$$\frac{F(s)}{s + M^2} = q_c \left[\frac{2\left(\frac{\pi}{\tau} \right)^2}{\left(\frac{2\pi}{\tau} \right)^2 + M^4} \right] \left[\frac{1}{s + M^2} - \frac{s}{s^2 + \left(\frac{2\pi}{\tau} \right)^2} + \frac{M^2}{\left(\frac{2\pi}{\tau} \right)} \frac{\frac{2\pi}{\tau}}{s^2 + \left(\frac{2\pi}{\tau} \right)^2} \right] \tag{43}$$

$$\mathcal{L}^{-1} \left\{ \frac{F(s)}{s + M^2} \right\} = q_c \left[\frac{2\left(\frac{\pi}{\tau} \right)^2}{\left(\frac{2\pi}{\tau} \right)^2 + M^4} \right] \left[e^{-M^2 T} - \cos\left(\frac{2\pi}{\tau} T \right) + \frac{M^2}{\left(\frac{2\pi}{\tau} \right)} \sin\left(\frac{2\pi}{\tau} T \right) \right]$$

▪ Dumped cyclic load

$$f(T) = q_c \left[-\beta e^{-\beta T} \sin\left(\frac{\pi}{\tau} \bullet T\right) + \frac{\pi}{\tau} e^{-\beta T} \cos\left(\frac{\pi}{\tau} \bullet T\right) \right]$$

$$F(s) = q_c \left[\frac{-\beta \frac{\pi}{\tau}}{(s+\beta)^2 + \left(\frac{\pi}{\tau}\right)^2} + \frac{\frac{\pi}{\tau}(s+\beta)}{(s+\beta)^2 + \left(\frac{\pi}{\tau}\right)^2} \right] = q_c \left[\frac{\frac{\pi}{\tau} s}{(s+\beta)^2 + \left(\frac{\pi}{\tau}\right)^2} \right]$$

$$\frac{F(s)}{s+M^2} = \left[\frac{\frac{\pi}{\tau}}{\beta^2 + \left(\frac{\pi}{\tau}\right)^2 - 2\beta M^2 + M^4} \right] \left\{ M^2 \frac{s+\beta}{(s+\beta)^2 + \left(\frac{\pi}{\tau}\right)^2} + \left[\frac{\beta^2 + \left(\frac{\pi}{\tau}\right)^2 - M^2 \beta}{\frac{\pi}{\tau}} \right] \frac{\frac{\pi}{\tau}}{(s+\beta)^2 + \left(\frac{\pi}{\tau}\right)^2} - M^2 \frac{1}{s+M^2} \right\} \tag{44}$$

$$\mathcal{L}^{-1}\left\{ \frac{F(s)}{s+M^2} \right\} = \left[\frac{\frac{\pi}{\tau}}{\beta^2 + \left(\frac{\pi}{\tau}\right)^2 - 2\beta M^2 + M^4} \right] \left\{ M^2 e^{-\beta T} \cos\left(\frac{\pi}{\tau} \bullet T\right) + \left[\frac{\beta^2 + \left(\frac{\pi}{\tau}\right)^2 - M^2 \beta}{\frac{\pi}{\tau}} \right] e^{-\beta T} \sin\left(\frac{\pi}{\tau} \bullet T\right) - M^2 e^{-M^2 T} \right\}$$